

RESEARCH ARTICLE

## Investigating cytotoxicity and the effect of Zn doped CeO<sub>2</sub> nanoparticles on tooth-damaging Streptococcus mutans bacteria

Somayeh Alirezaei<sup>1</sup>, Hamed Mahmoudi<sup>2</sup>, Soroush Ghodratizadeh<sup>3</sup>, Meysam Mohammadi Khah<sup>4,5</sup>, Azadehzeinab Titidej<sup>6\*</sup>

<sup>1</sup>Oral medicine dept. faculty of dentistry, Islamic Azad university of medical sciences, Tehran, Iran

<sup>2</sup>Resident of oral & maxillofacial surgery, School of dentistry, Tehran university of medical science, Tehran, Iran

<sup>3</sup>Department of Biochemistry, Faculty of Medicine, Urmia University of Medical Sciences, Urmia, Iran

<sup>4</sup>Department of Oral and Maxillofacial Surgery, School of Dentistry, Shahid Beheshti University of Medical Sciences, Tehran, Iran.

<sup>5</sup>Students' Research Committee, School of Dentistry, Shahid Beheshti University of Medical Sciences, Tehran, Iran

<sup>6</sup>Assistant professor, Oral & Maxillofacial Pathology Department, Qazvin University of Medical Sciences, Qazvin, Iran

### ARTICLE INFO

#### Article History:

Received 15 Sep 2022

Accepted 24 Oct 2022

Published 15 Feb 2023

#### Keywords:

Zn-CeO<sub>2</sub>-NP

Prosopis fracta

Streptococcus mutans

MTT assay

### ABSTRACT

The present study presents a simple method for the provision of pure and 5% zinc doped cerium oxide nanoparticles (Zn-CeO<sub>2</sub>-NP) through application of extraction from *prosopis fracta*. In the following, we determined the physical-chemical properties of the product by performance of FESEM, UV-Vis, PXRD, and EDX devices. The finding of PXRD and EDX thoroughly confirmed the existence of zinc inside the structure of CeO<sub>2</sub>-NP, while results of FESEM measured the particle sizes of pure and doped NP to be below 20 and 10 nm. An assessment was conducted on the cytotoxic performance of synthesized samples on colon cancer (HT-29) cell line through usage of MTT test. According to results, doping process caused an increase in the cytotoxic effect of CeO<sub>2</sub>-NP. The next section involved the evaluation of obtained antibacterial activity on *Streptococcus mutans* bacteria via micro-dilution, hence resulted in displaying higher antibacterial activity of doped NP than to pure CeO<sub>2</sub>-NP.

### How to cite this article

Alirezaei S., Mahmoudi H., Ghodratizadeh S., Mohammadi Khah M., Titidej A., Investigating cytotoxicity and the effect of Zn doped CeO<sub>2</sub> nanoparticles on tooth-damaging Streptococcus mutans bacteria. Nanomed Res J, 2023; 8(1): 16-23.

DOI: 10.22034/nmrj.2023.01.002

### INTRODUCTION

Cerium oxide (CeO<sub>2</sub>) is a member of lanthanide metal oxides that is known to contain the potential of exhibiting oxidation-reduction behaviors. Cerium oxide nanoparticles are the oxidized form of the rare cerium element that is capable of mimicking the activity of superoxide dismutase [1, 2]. This feature of cerium oxide is increased in nanoscale due to the provided greater ratio of surface area to volume. There are many potential applications available for nanoparticles in biomedicine that include endothelial cell protection, wound healing, anticancer applications, neuroprotection, and neuroregeneration [3, 4].

As it is known, the uncontrollable growth and reproduction of cells leads to the occurrence of cancer disease. Cells contain the ability to invade and move to other parts of the body and create tumors [5]. Although many efforts were made for the development of cancer treatment, which was successful in chemotherapy, yet the survival of cancer patients remains to be limited in many cases and therefore, it is necessary to find an applicable alternative treatment [6]. Size and dimensions, shape, surface structure, chemical composition, density, solubility, and surface charge are key items in characterizing the cytotoxic of NP [7-9]. Metal nanoparticles are responsible for the production of toxins in human tissues and cell cultures, which

\* Corresponding Author Email: [drtitidej@yahoo.com](mailto:drtitidej@yahoo.com)



This work is licensed under the Creative Commons Attribution 4.0 International License.

To view a copy of this license, visit <http://creativecommons.org/licenses/by/4.0/>.

expands the rate of inflammatory production likes cytokines and cause an increase in oxidative stress that ultimately results in the inducement of cell death. The absorbance of large nanoparticles by the nucleus and mitochondria is followed by the induction of mutation in DNA, demolition structure of mitochondrial, and finally cell death. Although there is a lack of full comprehension on accurate effect of NP on cancer cells, yet one of the possible mechanisms is assumed to be the extended production of reactive oxygen species (ROS) [10, 11]. The reaction of nanomaterials compound to cancer cells triggers activation of cellular defensive mechanism in order to minimize the induced damage. However, a stronger stimulation of ROS production by NP than antioxidant defensive capacity of cell results in cells annihilation pending the step of apoptotic cell. Since ROS stands as the potential source of nanoparticles cellular toxicity, oxidative stress can be considered as a suitable scale for comparing the toxic effects of different nanoparticles [12]. One of the exerted nanoparticles in industry and medicine is cerium oxide ( $\text{CeO}_2$ ) nanoparticle [13, 14].

Tooth decay is an infectious-microbial disease with the ability to dissolve and destroys dental calcareous tissues. Some of the complications of this disease are the loss of teeth, pain, and cosmetic defects [15, 16]. The main etiological factors known for tooth decay are *streptococci mutan* and *lactobacilli*. The technology of nanomaterials production initiated a tremendous revolution in antibacterial materials, that considered as major direction for the development of nano production and their numerous benefits on chemical materials [17].  $\text{CeO}_2$  nanoparticle contains a large number of antibacterial properties that led to its popularity as an antibacterial agent in various laboratory activities [18].

The biosynthesis of nanoparticles through the interaction of nanotechnology and biotechnology attracted the attention of many researchers due to the growing need for the development of environmentally compatible technologies for the synthesis of materials [19]. The aim of green technological projects is to minimize the rate of possible risks for humans and the environment. There are several advantages to the usage of biological methods when compared to chemical and physical procedures that include their compatibility with the environment, safety, requirement of shorter synthesizing time,

production of almost negligible industrial waste, and lack of exerting toxic chemicals throughout the manufacturing procedure. Considering how the physical and chemical synthesizing routes are expensive, dangerous, and time-consuming, there is a greater focus on the synthesis of nanoparticles through the application of natural resources such as plants and microbes, which is known as green synthesis [20]. In the last decay, the interest of many scientists was invested in the production of green nanoparticles by the exertion of plant origins due to the compatibility of these products with the environment and simplicity of their manufacturing process, as well as the achievement of high reaction speed and inhibition of microbial growth when compared to other routes [20]. Therefore, this research attempted to prepare pure and 5% Zn- $\text{CeO}_2$ -NP via a green way by utilization of *P. fructa*, and also evaluated the antibacterial and cytotoxic activities of prepared nanoparticles.

## EXPERIMENTAL

### Prepare of pure and Zn- $\text{CeO}_2$ -NP

The bark powder of *P. fructa* was weighed, and then added to distilled water (DW) with ratio 1 to 10, after that shaken for 20 h at 150 rpm. Final solution was filtered using Whatman paper. In the next step, 20 mL from *Prosopis fructa* extract was added to two Erlenmeyer's, and were volumed up to 100 mL by addition of DW, and positioned in water bath with 70 °C temperature. In next stage, 100 mL of solutions containing  $\text{Ce}(\text{NO}_3)_3 \cdot 6\text{H}_2\text{O}$  (1 mM, Merck) and  $\text{Zn}(\text{NO}_3)_2 \cdot 6\text{H}_2\text{O}$  (Merck, according to formula of  $\text{Zn}_{1-x}\text{Ce}_x\text{O}_2$ , while percentages of zinc nitrate is 0 and 5) were added to extract solution and stirred for 5 h. These solutions were dried in 85 °C during 10 h, and eventually the resulting powders were calcined with furnace of 400 °C in 1:30 h.

### Characterization of NP

The characteristics of synthesized NP were through the results of different technics. The crystalline nature was survived through PXRD analysis (Netherlands, PANalyticalX'Pert PRO MPD system, Cu K $\alpha$ ). The absorption spectroscopy of samples determined using UV-Vis (Halo DB-20 UV-Vis double beam), while functional groups of prepared samples were conducted using FT-IR analysis (Spectrum One, PerkinElmer, Waltham, MA, USA). The surface morphology and particle size distribution of NP was determined via FESEM

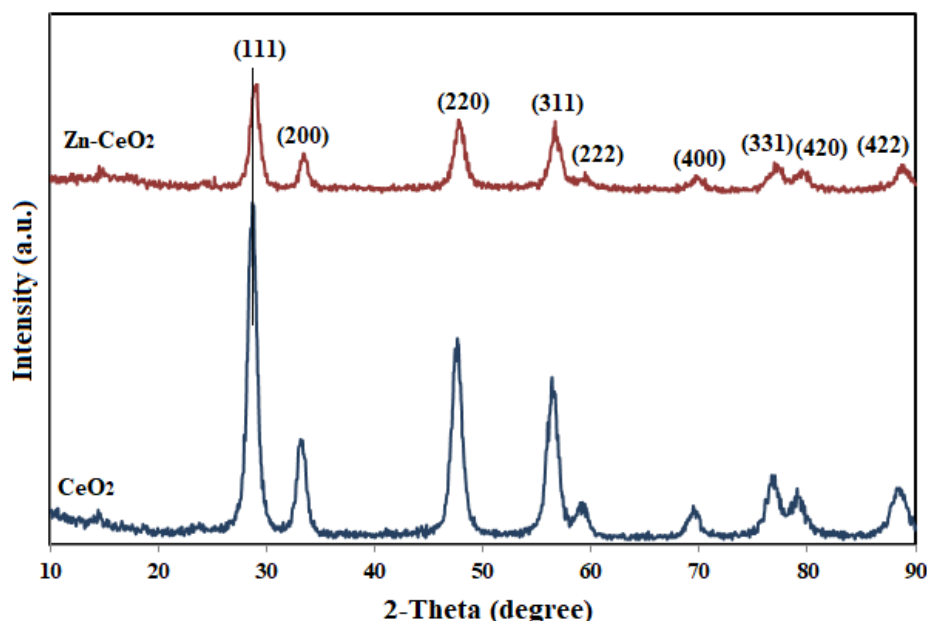


Fig. 1. PXRD spectra of pure and 5% Zn-CeO<sub>2</sub>-NP.

(MIRA3 TESCAN, Czech) analyses.

#### Antibacterial section

##### Assessment of the Inhibitory Activity

In the following, we performed a well-diffusion trial to collect data on the inhibitory performance of pure and doped NP towards *Streptococcus mutans* bacteria. For this purpose, the streaking technic was exerted to inoculate the experimental bacteria into the sterile 96-well microplate. Begging, subsequent to preparing the serial concentrations of NP (1.56, 3.12, 6.25, 12.5, 25, 50, 100, 200, and 400 µg/mL), sample (100 µL) was poured into the microplate shafts. After that, Mueller Hinton Broth (90 µL) were added to the microplate shafts to contained the NP. After cultivation, microplates were incubated at 37 °C for 24 h in an incubator. Subsequent to incubation period, the turbidity of the shafts was assigned through ELISA device at the wavelength of 620 nm. The lowest concentration of NP that lacked any bacterial growth (induction of zero turbidity by bacterial growth) was survey as MIC. In following, minimum bactericidal concentration (MBC) determined according Akbarizadeh *et al* work [17].

#### Cytotoxic performance

##### MTT assay

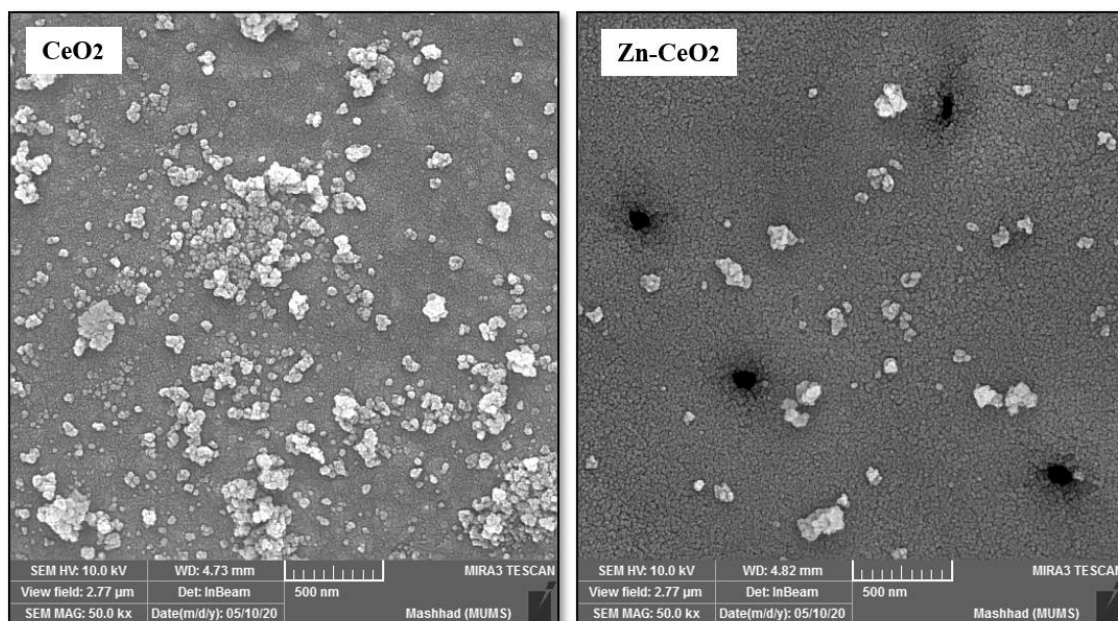
For this section, human colon cancer (HT-29) cell line was prepared from Tehran Pasteur

Institute, Iran. The cell culture process was done based on Hamidian *et al* work [14]. In following, the amount of 100 cells per 4 microliters of culture medium that contained the number of 10 cells fixed in a 96-well plate. Subsequent to 24 h of incubation, the concentrations of 1-1000 µg/mL of NP were added to the cells to conduct incubation for 24 h. Then, 20 µL of MTT with a concentration of 5 mg/mL was added to each well to be incubated again in un-light place for the duration of 4 h. In the following, the culture medium containing MTT was removed. After 15 min of incubation, we read the optical absorbance of each well by the usage of an ELISA device. The outcomes were reported in form of cell survival rate and IC<sub>50</sub> based on the concentration curve (µg/mL). Each of these experiments was repeated in triplicate.

## RESULTS AND DISCUSSION

### PXRD

The PXRD graphs of pure and 5% Zn-CeO<sub>2</sub>-NP shown in Fig. 1. The PXRD graph of CeO<sub>2</sub>-NP exhibited their cubic phase by pointing out peaks at  $2\theta = 28.13, 33.26, 47.84, 56.25, 59.49, 69.97, 76.49, 79.29, \text{ and } 88.50^\circ$ , which is consistent with planes of (111), (200), (220), (311), (222), (400), (331), (420), and (422) planes; (JCPDS code: 81-0792) [13]. As seen in Fig. 1, the intensity of all peaks of doped NP was dropped than to peaks of CeO<sub>2</sub>-NP after the doping of zinc to CeO<sub>2</sub>-NP structure. A slight

Fig. 2. FESEM images of pure and 5% Zn-CeO<sub>2</sub>-NP.

shift in position (111) peak was showed at PXRD peak of Zn-CeO<sub>2</sub>-NP, which expresses the insert of zinc ions in CeO<sub>2</sub> lattice. Obtained crystallite size of NP by application of Scherrer's equation [21] were 19.23, and 8.14 nm for pure and 5% Zn-CeO<sub>2</sub>-NP, respectively. This decrease in crystal size of Zn-CeO<sub>2</sub>-NP is because of the lower ionic radius of Zn ion (0.74 Å) when compared to Ce ion (1.034 Å).

#### FESEM and EDX

The results of FESEM analysis demonstrated the structural data of prepared pure and 5% Zn-CeO<sub>2</sub>-NP. In conformity to Fig. 2, size of CeO<sub>2</sub> particles was reported to be below 20 nm. In additional, observations were indicative of a decrease in the size of doped particles as a result of adding zinc into the crystalline lattice of CeO<sub>2</sub>. As it was mentioned in PXRD part, this case is because of lower ionic radius of zinc ion when compared to cerium ion. The EDX outcomes of NP approve the satisfying entry of zinc in structure of CeO<sub>2</sub>-NP. Based on Fig. 3, percentages of existing zinc at the cases of pure and 5% Zn-CeO<sub>2</sub>-NP were 0 and 4.64%, respectively. It approved the lack of each impurity all the construction of NP.

#### Raman

The Raman graphs of pure and 5% Zn-CeO<sub>2</sub>-NP are presented in Fig. 4. Accordingly, the observed active band of F2g at 459 cm<sup>-1</sup> throughout graph

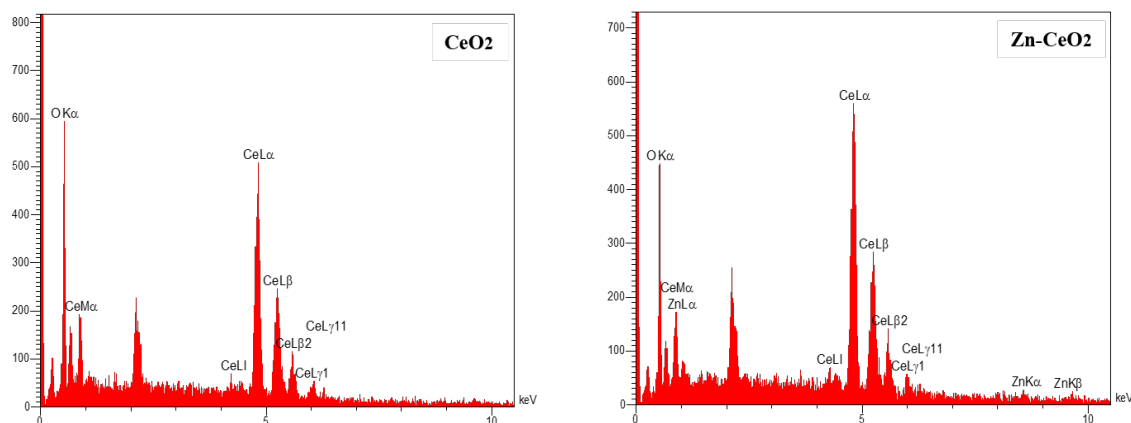
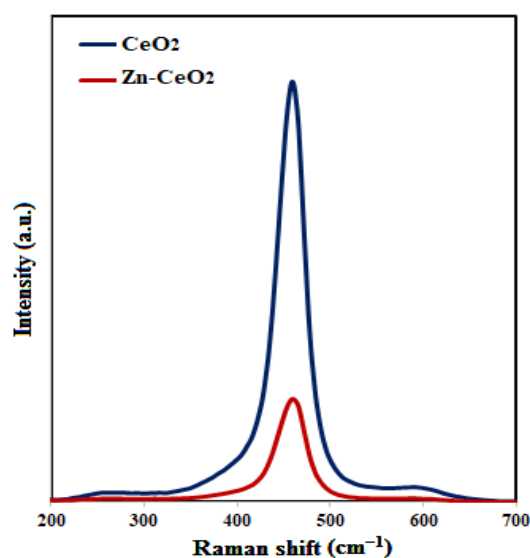
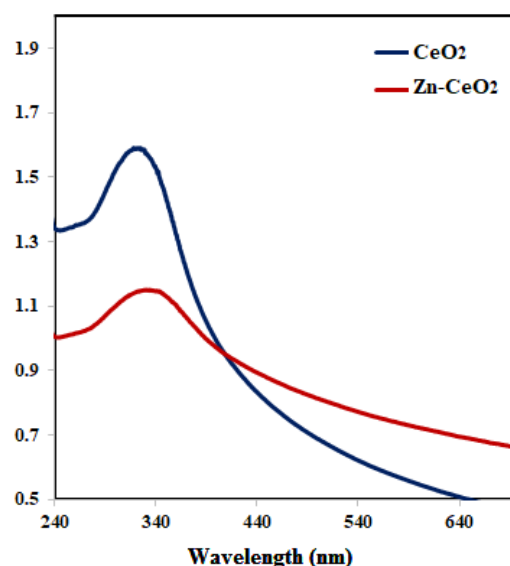
of CeO<sub>2</sub> may be related to fluorite structure for CeO<sub>2</sub>, which once again validates FCC structure of prepared nanoparticles. So, it can be assumed that the vibrational mode is almost independent of the ionic mass of CeO<sub>2</sub> by the movement of O atoms. In conformity to Fig. 4, increasing the doped percentage of Zn into the structure of CeO<sub>2</sub> caused a decrease in the intensity of 459 cm<sup>-1</sup> peak [14]. The formation of CeO<sub>2</sub> was in total agreement with the results of PXRD pattern.

#### UV-Vis

Fig. 5 displays UV-visible absorption graph of pure and 5% Zn-CeO<sub>2</sub>-NP, which is primarily used to obtain the band gap of materials, and also exerted to record. The induced alterations in the energy band structure of CeO<sub>2</sub> upon the doping of Zn. As shown in Fig. 5(A), optical absorption depicted absorption peaks at regions of 343, 335, 328, and 321 nm that were related to belonged to pure and 5% Zn-CeO<sub>2</sub>-NP, respectively. Apparently, increasing the doping concentration of Zn caused a blue shift in of absorption spectra to lower wavelengths, which is related to the induced alteration in the amount of optical band gap [14].

#### Antibacterial assay

According to the results of assessing MIC and MBC, we observed growth inhibiting and bactericidal effects of pure and doped nanoparticles

Fig. 3. EDX images of pure and 5% Zn-CeO<sub>2</sub>-NP.Fig. 4. Raman graphs of pure and 5% Zn-CeO<sub>2</sub>-NP.Fig. 5. (A) UV-Vis spectra of pure and 5% Zn-CeO<sub>2</sub>-NP.

on *S. mutans* as the accountable bacteria for tooth decay. The doping of Zn-CeO<sub>2</sub> NP caused an increase in the inhibitory activity of CeO<sub>2</sub> NP (Fig. 6), which is confirmed by the data of Table 1.

Previous studies reported the important role of particles size and shape for antibacterial feature of NP. For instance, a decrement in particle size can result in the formation of suitable interactions with bacteria and empower this feature. Decreasing the size of particles can extend the rate of released ions from the surface, which is the main mechanism of providing stronger antibacterial properties [22]. Some of the other fundamental mechanisms include damaging the cell membrane, production of reactive oxygen species, and attacking the cells

by ions that is followed by damaging the ATP products and inhibition of DNA replication [23].

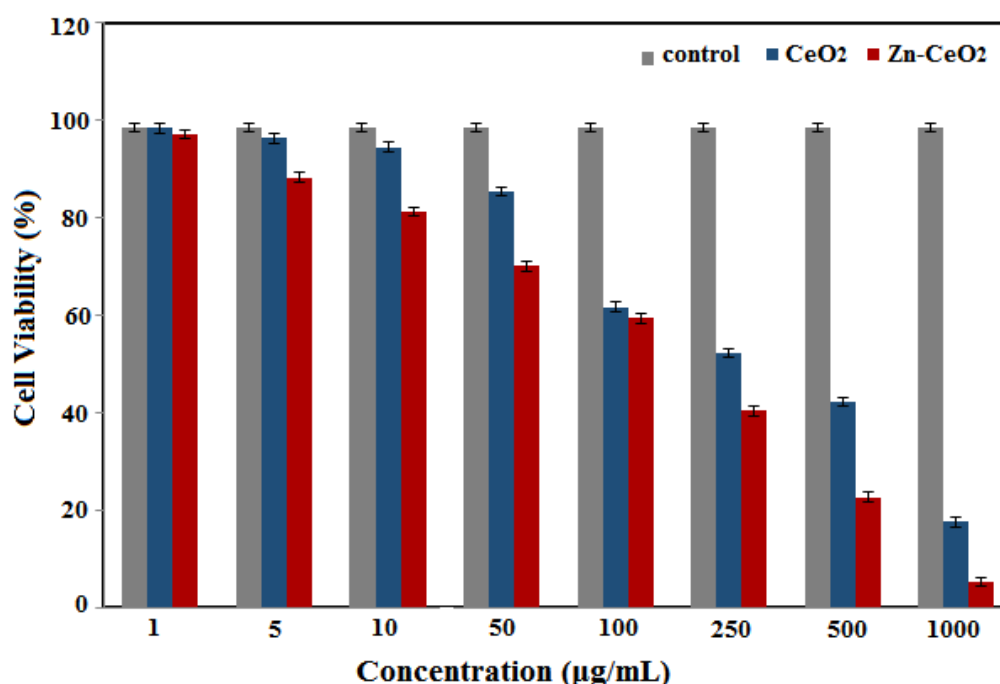
#### Anticancer assay

Cerium oxide is a metal nanoparticle with the abilities to induce toxic effects on cancer cells, inhibit invasion, sensitizes cells to chemotherapy and radiation therapy, protect reactive oxygen species (ROS), and prevent the occurrence of metastasis [2]. We attempted to study the cytotoxicity of cerium oxide nanoparticles at different concentrations in colon cancer (HT-29) cell line. According to results, pure and doped nanoparticles displayed the greatest toxicity in the concentrations of 500 and 250 µg/mL, respectively,



Table 1. MIC and MBC results of pure and 5% Zn-CeO<sub>2</sub>-NP on *S. mutans* bacteria

Nanoparticles	<i>Streptococcus mutans</i> bacteria	
	MIC (µg/mL)	MBC (µg/mL)
CeO <sub>2</sub>	25	6.25
Zn-CeO <sub>2</sub>	12.5	3.12

Fig. 7. Cytotoxic effect of pure and 5% Zn-CeO<sub>2</sub>-NP on HT-29 cell line after 24 h treatment

while exhibiting a significant difference with the control cells along with a dose-dependent toxicity effect (Fig. 7).

In general, increasing the applied concentration of nanoparticles can heighten their chances of entering the cells and inducing their toxic effects through the progression of oxidative stress (production of toxic oxygen radicals). Oxidative stress disrupts the occurrence of intracellular homeostasis and interactions with cellular macromolecules such as DNA, proteins, and lipids. In addition, this phenomenon can cause the breakage of double-stranded DNA and lead to the death of cancer cells.

Various studies investigated the cytotoxic of CeO<sub>2</sub>-NP on various cell lines. The work of M. Pešić

*et al.* investigated the cytotoxic impact of CeO<sub>2</sub> NP on several types of cancer and normal cell lines and also evaluated the properties of intracellular redox changes. Their results indicated the effect of CeO<sub>2</sub> NP on increasing the rate of cell death and active oxygen species, while the highest sensitivity was detected in 518A2 and HT-29 cells with high IC50 values [24]. Saikat Jana *et al.*, conducted research on the toxicity effect of CeO<sub>2</sub> NP on HCT-15 cell line and observed a dose-dependent significant increase in both ROS and lipid peroxidation as the indicators of oxidative stress and cytotoxicity [25]. Another mechanism for the cytotoxic effects of cerium oxide nanoparticles is release of cytochrome c and the activation of caspase 3 and 9, which

increases the apoptosis of cancer cells by targeting mitochondria and initiating mitochondrial cell death without causing any chemical changes [26]. Nevertheless, the results of our study exhibited the ability of zinc metal doping process to increase the cytotoxic activity of cerium oxide nanoparticles. Therefore, it is useful to conduct more assessments on the biological properties of doped nanoparticles to determine the medical importance of these products.

## CONCLUSION

In summary, pure and 5% Zn-CeO<sub>2</sub>-NP were synthesized by the usage of *P. fraxa* extract to explore their physic-chemical, antibacterial, cytotoxic properties through the performance of various methods such as FESEM, PXRD, Raman, EDX, and UV-Vis spectroscopy. The average particle size was presented by Debye-Scherrer equation and FESEM images, which achieved very close outcomes. The data of EDX, PXRD, and Raman analyses presented the existence of a single phase, highly pure, and cubic fluorite structure for the synthesized pure and doped NP. According to our observations, Zn-CeO<sub>2</sub>-NP exhibited proper antibacterial and cytotoxic performances when compared to the results of pure CeO<sub>2</sub>-NP.

## CONFLICT OF INTEREST

The authors declare no conflict of interest

## REFERENCES

- Singh, K.R., et al., Cerium oxide nanoparticles: properties, biosynthesis and biomedical application. RSC advances, 2020. 10(45): p. 27194-27214. <https://doi.org/10.1039/D0RA04736H>
- Nyoka, M., et al., Synthesis of cerium oxide nanoparticles using various methods: implications for biomedical applications. Nanomaterials, 2020. 10(2): p. 242. <https://doi.org/10.3390/nano10020242>
- Khan, I., K. Saeed, and I. Khan, Nanoparticles: properties, applications and toxicities. Arab J Chem 12: 908. 2017. <https://doi.org/10.1016/j.arabjc.2017.05.011>
- Miri, A., S. Akbarpour Birjandi, and M. Sarani, Survey of cytotoxic and UV protection effects of biosynthesized cerium oxide nanoparticles. Journal of Biochemical and Molecular Toxicology, 2020. 34(6): p. e22475. <https://doi.org/10.1002/jbt.22475>
- Martin, T.A. and W.G. Jiang, Loss of tight junction barrier function and its role in cancer metastasis. Biochimica et Biophysica Acta (BBA)-Biomembranes, 2009. 1788(4): p. 872-891. <https://doi.org/10.1016/j.bbame.2008.11.005>
- Richter, U., et al., Adhesion of small cell lung cancer cells to E- and P-selectin under physiological flow conditions: implications for metastasis formation. Histochemistry and cell biology, 2011. 135(5): p. 499-512. <https://doi.org/10.1007/s00418-011-0804-4>
- Jin, C., et al., Application of nanotechnology in cancer diagnosis and therapy-a mini-review. International Journal of Medical Sciences, 2020. 17(18): p. 2964. <https://doi.org/10.7150/ijms.49801>
- Zhou, L., et al., Analysis of invasion-metastasis in pancreatic cancer: correlation between the expression and arrangement of tight junction protein-2 and cell dissociation in pancreatic cancer cells. Molecular medicine reports, 2010. 3(1): p. 149-153. <https://doi.org/10.3892/mmr.00000232>
- Bornholdt, J., et al., The level of claudin-7 is reduced as an early event in colorectal carcinogenesis. BMC cancer, 2011. 11(1): p. 1-9. <https://doi.org/10.1186/1471-2407-11-65>
- Gavas, S., S. Quazi, and T.M. Karpiński, Nanoparticles for cancer therapy: Current progress and challenges. Nanoscale Research Letters, 2021. 16(1): p. 1-21. <https://doi.org/10.1186/s11671-021-03628-6>
- Mahapatro, A. and D. Singh, Biodegradable Nanoparticles Are Excellent Vehicle for Site Directed. Vivo.
- Sandin, L.C., et al., Local CTLA4 blockade effectively restrains experimental pancreatic adenocarcinoma growth in vivo. Oncoimmunology, 2014. 3(1): p. e27614. <https://doi.org/10.4161/onci.27614>
- Khatami, M., et al., Nickel-doped cerium oxide nanoparticles: green synthesis using stevia and protective effect against harmful ultraviolet rays. Molecules, 2019. 24(24): p. 4424. <https://doi.org/10.3390/molecules24244424>
- Hamidian, K., et al., Doped and un-doped cerium oxide nanoparticles: Biosynthesis, characterization, and cytotoxic study. Ceramics International, 2021. 47(10): p. 13895-13902. <https://doi.org/10.1016/j.ceramint.2021.01.256>
- Caufield, P.W., Y. Li, and A. Dasanayake, Dental caries: an infectious and transmissible disease. Compendium of continuing education in dentistry (Jamesburg, NJ: 1995), 2005. 26(5 Suppl 1): p. 10-16.
- Taylor, G.W., M.C. Manz, and W.S. Borgnakke, Diabetes, periodontal diseases, dental caries, and tooth loss: a review of the literature. Compendium of continuing education in dentistry (Jamesburg, NJ: 1995), 2004. 25(3): p. 179-84, 186.
- Akbarzadeh, M.R., M. Sarani, and S. Darjani, Study of antibacterial performance of biosynthesized pure and Ag-doped ZnO nanoparticles. Rendiconti Lincei. Scienze Fisiche e Naturali, 2022. 33(3): p. 613-621. <https://doi.org/10.1007/s12210-022-01079-4>
- Farias, I.A.P., C.C.L.d. Santos, and F.C. Sampaio, Antimicrobial activity of cerium oxide nanoparticles on opportunistic microorganisms: a systematic review. BioMed research international, 2018. 2018. <https://doi.org/10.1155/2018/1923606>
- Ahmed, S.F., et al., Green approaches in synthesising nanomaterials for environmental nanobioremediation: Technological advancements, applications, benefits and challenges. Environmental Research, 2022. 204: p. 111967. <https://doi.org/10.1016/j.envres.2021.111967>
- Sharma, D., S. Kanchi, and K. Bisetty, Biogenic synthesis of nanoparticles: a review. Arabian journal of chemistry, 2019. 12(8): p. 3576-3600. <https://doi.org/10.1016/j.arabjc.2015.11.002>
- Sarani, M., et al., Study of in vitro cytotoxic performance of biosynthesized  $\alpha$ -Bi<sub>2</sub>O<sub>3</sub> NPs, Mn-doped and Zn-doped Bi<sub>2</sub>O<sub>3</sub> NPs against MCF-7 and HUVEC cell lines. Journal

- of Materials Research and Technology, 2022. 19: p. 140-150.  
<https://doi.org/10.1016/j.jmrt.2022.05.002>
22. Guzman, M., J. Dille, and S. Godet, Synthesis and antibacterial activity of silver nanoparticles against gram-positive and gram-negative bacteria. *Nanomedicine: Nanotechnology, biology and medicine*, 2012. 8(1): p. 37-45.  
<https://doi.org/10.1016/j.nano.2011.05.007>
23. Kouhbanani, M.A.J., et al., The inhibitory role of synthesized Nickel oxide nanoparticles against Hep-G2, MCF-7, and HT-29 cell lines: the inhibitory role of NiO NPs against Hep-G2, MCF-7, and HT-29 cell lines. *Green Chemistry Letters and Reviews*, 2021. 14(3): p. 444-454.  
<https://doi.org/10.1080/17518253.2021.1939435>
24. Pešić, M., et al., Anti-cancer effects of cerium oxide nanoparticles and its intracellular redox activity. *Chemico-biological interactions*, 2015. 232: p. 85-93.  
<https://doi.org/10.1016/j.cbi.2015.03.013>
25. Jana, S., et al., Chaudhury KJJoNR. Redox-active nanoceria depolarize mitochondrial membrane of human colon cancer cells, 2014. 16(6): p. 2441.  
<https://doi.org/10.1007/s11051-014-2441-z>
26. Arya, A., et al., Cerium oxide nanoparticles prevent apoptosis in primary cortical culture by stabilizing mitochondrial membrane potential. *Free radical research*, 2014. 48(7): p. 784-793.  
<https://doi.org/10.3109/10715762.2014.906593>

